

Analytic Photometric Redshift Estimator for Type Ia Supernovae From the Large Synoptic Survey Telescope

Yun Wang^{1,2*}, E. Gjergo³, and S. Kuhlmann³

¹*Infrared Processing and Analysis Center, California Institute of Technology, 770 South Wilson Avenue, Pasadena, CA 91125*

²*Homer L. Dodge Department of Physics & Astronomy, Univ. of Oklahoma, 440 W Brooks St., Norman, OK 73019, U.S.A.*

³*Argonne National Laboratory, 9700 South Cass Avenue, Lemont, IL 60439, USA*

9 June 2019

ABSTRACT

Accurate and precise photometric redshifts (photo- z 's) of Type Ia supernovae (SNe Ia) can enable the use of SNe Ia, measured only with photometry, to probe cosmology. This dramatically increases the science return of supernova surveys planned for the Large Synoptic Survey Telescope (LSST). In this paper we describe a significantly improved version of the simple analytic photo- z estimator proposed by Wang (2007) and further developed by Wang, Narayan, and Wood-Vasey (2007). We apply it to 55,422 simulated SNe Ia generated using the SNANA package with the LSST filters. We find that the estimated errors on the photo- z 's, $\sigma_{z_{\text{phot}}}/(1+z_{\text{phot}})$, can be used as filters to produce a set of photo- z 's that have high precision, accuracy, and purity. Using SN Ia colors as well as SN Ia peak magnitude in the i band, we obtain a set of photo- z 's with 2 percent accuracy (with $\sigma(z_{\text{phot}} - z_{\text{spec}})/(1+z_{\text{spec}}) = 0.02$), a bias in z_{phot} (the mean of $z_{\text{phot}} - z_{\text{spec}}$) of -9×10^{-5} , and an outlier fraction (with $|(z_{\text{phot}} - z_{\text{spec}})/(1+z_{\text{spec}})| > 0.1$) of 0.23 percent, with the requirement that $\sigma_{z_{\text{phot}}}/(1+z_{\text{phot}}) < 0.01$. Using the SN Ia colors only, we obtain a set of photo- z 's with similar quality by requiring that $\sigma_{z_{\text{phot}}}/(1+z_{\text{phot}}) < 0.007$; this leads to a set of photo- z 's with 2 percent accuracy, a bias in z_{phot} of 5.9×10^{-4} , and an outlier fraction of 0.32 percent.

Key words: cosmology: observations, distance scale

1 INTRODUCTION

The use of Type Ia supernovae (SNe Ia) as cosmological standard candles is a corner stone of modern cosmology (Riess et al. 1998; Perlmutter et al. 1999). We can expect a dramatic increase in the number of SNe Ia that can be used to measure cosmological distances in the coming years and decades. Thousands of SNe Ia are expected from the Dark Energy Survey (DES) (Bernstein et al. 2012), and hundreds of thousands of SNe Ia are expected from Large Synoptic Survey Telescope (LSST) (Abell et al. 2009).¹

The majority of the SNe Ia from LSST will only have photometry, and will not have spectroscopic redshifts, due to the expensive resources required to obtain follow-up spectroscopy. Fortunately, the redshifts of the SNe Ia can be estimated using multi-band photometry (these approximate redshifts are called photometric redshifts, or photo- z 's). SNe Ia with sufficiently accurate and precise photo- z 's can be used for probing cosmology. This would dramatically increase the science return of supernova surveys planned for LSST. Accurate photo- z 's can also enhance the ability of observers to accurately target high redshift SNe Ia for spectroscopy, allowing

flexibility and optimization in survey design for Stage III and Stage IV dark energy projects (Albrecht et al. 2006).

In this paper, we build on the previous work by Wang (2007) and Wang, Narayan, & Wood-Vasey (2007), and present a simple analytic photo- z estimator. We apply this photo- z estimator to 55,422 simulated SNe Ia generated using the SNANA package with the LSST filters. We present our method in Sec.2, describe the simulation of LSST SNe Ia in Sec.3, show our results in Sec.4, and discuss our findings in Sec.5.

2 THE METHOD

The analytic photo- z estimator for SNe Ia proposed by Wang (2007) is empirical, model independent (no templates used), and uses observables that reflect the properties of SNe Ia as calibrated standard candles. It was developed using the SN Ia data released by the Supernova Legacy Survey (Astier et al. 2006).

2.1 The Prototype Photo- z Estimator

The prototype photo- z estimator we use here was developed in Wang (2007) and Wang, Narayan, and Wood-Vasey (2007). This

* E-mail: wang@ipac.caltech.edu

¹ <http://www.lsst.org/lsst/science>

estimator uses the fluxes in *griz* (or *riz*) at the epoch of *i* maximum flux to make an effective K-correction to the *i* flux. The first estimate of redshift is given by

$$z_{\text{phot}}^0 = c_1 + c_2 g_f + c_3 r_f + c_4 i_f + c_5 z_f + c_6 i_f^2 + c_7 i_f^3 \quad (1)$$

where $g_f = 2.5 \log(f_g)$, $r_f = 2.5 \log(f_r)$, $i_f = 2.5 \log(f_i)$, and $z_f = 2.5 \log(f_z)$, and f_g, f_r, f_i, f_z are fluxes in counts, normalized to some fiducial zeropoint, in *griz* at the epoch of *i* maximum flux.

Next, the photo-z estimator calibrates each SN Ia in its estimated rest-frame using

$$\Delta i_{15} = 2.5 \log(f_i^{15d} / f_i), \quad (2)$$

where f_i^{15d} is the *i* band flux at 15 days after the *i* flux maximum in the estimated rest-frame, corresponding to the epoch of $\Delta t^{15d} = 15(1 + z_{\text{phot}}^0)$ days after the epoch of *i* flux maximum.

The final estimate for the photometric redshift is given by

$$z_{\text{phot}} = \sum_{i=1}^8 c_i p_i, \quad (3)$$

where the data vector $\mathbf{p} = \{1, g_f, r_f, i_f, z_f, i_f^2, i_f^3, \Delta i_{15}\}$. The coefficients c_i ($i=1,2,\dots,8$) are found by using a training set of SNe Ia with *griz* (or *riz*, for which $c_2 = 0$) lightcurves and measured spectroscopic redshifts. The jackknife technique (Lupton 1993) is used to estimate the mean and the covariance matrix of c_i .

2.2 Photo-z Estimator Applied to LSST Filters

For application to SNe Ia from LSST with photometry only, we have simplified and modified the analytic photo-z estimator for easier application and better performance as follows:

- (1) Instead of using the fluxes in all filters except *i* at the epoch of *i* maximum flux to make an effective K-correction to the *i* flux, we just use the peak magnitudes in all filters for each SN to construct an indicator of the spectral shape of the SN.
- (2) We add 2nd order terms in the colors for improved accuracy and precision of the estimator.
- (3) We replace i_{15} with i_{12} , to increase the sample size.

The key to obtaining a set of reliable photo-z's for SNe is to exclude the SNe that are inferred to have unreliable photo-z estimates based on the photometry data alone. We make a first cut in SNe to be used as follows:

- (1) Exclude the few SNe that have no *i*-band photometry. This is necessary since we use the *i* magnitude at maximum light in estimating the photo-z's.
- (2) Exclude SNe that have measured flux uncertainties at maximum light in any passband that exceeds 0.2 magnitude. This is useful in reducing the number of outliers with $|(z_{\text{phot}} - z_{\text{spec}})/(1 + z_{\text{spec}})| > 0.1$.
- (3) Exclude SNe that do not have *i*-band lightcurve data that extends to 12 days after maximum light in the estimated SN rest-frame. This enables the refinement of the photo-z estimated using the fluxes at maximum light alone.

We then apply the photo-z estimator as follows:

- (1) Divide the SNe according to the passbands in which the SN magnitudes at maximum light are available.
- (2) For each set of SNe with photometry in the same passbands, construct the initial photo-z estimate given by

$$z_{\text{phot}}^0 = c_1 + \sum_{j=1}^{n-1} c_{j+1} (m_{p,j} - m_{p,j+1})$$

$$+ \sum_{j=1}^{n-1} c_{n+j} (m_{p,j} - m_{p,j+1})^2 + c_{2n} i_p + c_{2n+1} i_p^2 + c_{2n+2} i_p^3 \quad (4)$$

where $m_{p,j}$ is the magnitude at maximum light in the *j*-th passband, i_p is the magnitude at maximum light in the *i* band, n is the number of filters or passbands with available photometry, and $\{c_j\}$, $j = 1, 2, \dots, 2n + 2$, are the coefficients to be estimated from using the training set of SNe with spectroscopic redshifts.

(3) Next, calibrate each SN Ia in its estimated rest-frame using

$$\Delta i_{12} = i_{12d} - i_p \quad (5)$$

where i_{12d} is the *i* band magnitude at 12 days after the *i* maximum light in the estimated rest-frame, corresponding to the epoch of $\Delta t^{12d} = 12(1 + z_{\text{phot}}^0)$ days after the epoch of *i* maximum light.

The final estimate for the photometric redshift is given by

$$z_{\text{phot}} = \sum_{j=1}^{2n+3} c_j p_j, \quad (6)$$

where the data vector $\mathbf{p} = \{1, (m_{p,1} - m_{p,2}), (m_{p,2} - m_{p,3}), \dots, (m_{p,n-1} - m_{p,n}), (m_{p,1} - m_{p,2})^2, (m_{p,2} - m_{p,3})^2, \dots, (m_{p,n-1} - m_{p,n})^2, i_p, i_p^2, i_p^3, \Delta i_{12}\}$. The coefficients c_j ($j = 1, 2, \dots, 2n + 3$) are found by using a training set of SNe Ia with lightcurves in n passbands and measured spectroscopic redshifts. We use the same modified jackknife technique as in Wang, Narayan, and Wood-Vasey (2007) to estimate the mean and the covariance matrix of c_j (see Sec. 4).

2.3 Photo-z Estimator Using Colors Only

Since our ultimate goal is to use SNe Ia with photometry to probe cosmology, it is desirable to have a photo-z estimator that does *not* use the *i* band flux information, to avoid any double counting of distance information. We arrive at such a photo-z estimator simply by omitting the last 4 terms in Eq.(6).

Thus the simplified photo-z estimator that uses colors only is given by

$$z_{\text{phot}}^c = c_1 + \sum_{j=1}^{n-1} c_{j+1} (m_{p,j} - m_{p,j+1}) + \sum_{j=1}^{n-1} c_{n+j} (m_{p,j} - m_{p,j+1})^2 \quad (7)$$

where $m_{p,j}$ is the magnitude at maximum light in the *j*-th passband, n is the number of filters or passbands with available photometry, and $\{c_j\}$, $j = 1, 2, \dots, 2n - 1$, are the coefficients to be estimated from using the training set of SNe with spectroscopic redshifts.

3 SIMULATION OF DATA

We use a set of 55,422 simulated SNe with photometric data including magnitude uncertainties generated using the SNANA package with the LSST filters. We do not include LSST Photon Simulator effects or systematic bandpass zeropoint shifts at present. We have applied 0.005 mag of smearing to the bandpass zeropoints, to somewhat mock up effects in the Photon Simulator.

Only 55,414 of these simulated SNe have peak *i* mags, and

only 49,993 have i band lightcurves. Requiring that the i lightcurve data include info of the i peak and extend to 12 days in the estimated SN restframe, and that all the peak magnitudes have errors less than 0.2 magnitudes, we arrive at a sample of 29,702 simulated SNe.

We now describe our Type Ia SN light curve simulations in greater technical detail. We employ the SNANA package (Kessler et al. 2009b) to simulate the light curves using the SALT2 Type Ia SN model. The SNANA package was first used by the LSST collaboration to forecast SN observations (Abell et al. 2009), and has been used extensively by the SDSS collaboration (Kessler et al. 2009a), to forecast observations for the Dark Energy Survey (Bernstein et al. 2012), and for many other systematic studies for supernova cosmology. The specific SALT2 model used is the extended version of the Guy 2010 model (Guy et al. 2007, 2010). The SALT2 model rest-frame flux $F(p, \lambda)$ as a function of phase p and wavelength λ , is given in equation 8. The two spectral time series, M_0 and M_1 , and the color law CL are part of the specific SALT2 input model. The parameters x_0, x_1, c , are randomly drawn from distributions that have been fit previously to Type Ia SN data including the effects of dust extinction. Given these parameters the rest-frame flux as a function of phase is available for use. The redshift is likewise randomly drawn from a previously measured distribution, and the observer-frame flux is integrated with the LSST filter transmissions.

$$F(p, \lambda) = x_0[M_0(p, \lambda) + x_1 M_1(p, \lambda)]e^{-cCL(\lambda)}. \quad (8)$$

4 RESULTS

4.1 Photo-z's using SN Ia colors and i band peak flux

We use a slightly modified version of the jackknife technique (Lupton 1993) to estimate the mean and the covariance matrix of c_j . From the training set containing N SNe Ia, we extract N subsamples each containing $N - 1$ SNe Ia by omitting one SN Ia. The coefficients $c_j^{(s)}$ ($j = 1, 2, \dots, 2n + 3$) for the s -th subsample are found by a maximum likelihood analysis matching the predictions of Eq. (6) with the spectroscopic redshifts.

The mean of the coefficients c_j ($j = 1, 2, \dots, 2n + 3$) are given by

$$\langle c_j \rangle = \frac{1}{N} \sum_{s=1}^N c_j^{(s)}. \quad (9)$$

Note that this is related to the usual “bias-corrected jackknife estimate” for c_i, c_i^J , as follows:

$$c_j^J \equiv c_j^N + (N - 1)(c_j^N - \langle c_j \rangle), \quad (10)$$

where c_j^N are estimated from the entire training set (with N SNe Ia). Wang, Narayan, & Wood-Vasey (2007) found that for small training sets (with $N < 20$) that include SNe Ia at $z \sim 0$, c_j^J give biased estimates of c_j by giving too much weight to the SN Ia with the smallest redshift. For training sets not including nearby SNe Ia, $\langle c_j \rangle$ and c_j^J are approximately equal. We have chosen to use $\langle c_j \rangle$ from Eq. (9) as the mean estimates for c_j to avoid biased z_{phot} for SNe Ia at z close to zero (Wang, Narayan, & Wood-Vasey 2007).

The covariance matrix of c_j ($j = 1, 2, \dots, 2n + 3$) are given by

$$\text{Cov}(c_i, c_j) = \frac{N - 1}{N} \sum_{s=1}^N \left(c_i^{(s)} - \langle c_i \rangle \right) \left(c_j^{(s)} - \langle c_j \rangle \right) \quad (11)$$

Using $z_{\text{phot}} = \sum c_j p_j$, we find that $\Delta z_{\text{phot}} = \sum p_j \Delta c_j$, since the uncertainty in z_{phot} is dominated by the uncertainty in c_j . Therefore estimated error in z_{phot} is

$$dz_{\text{phot}} = \left\{ \sum_{i=1}^{2n+3} \sum_{j=1}^{2n+3} [p_i] \text{Cov}(c_i, c_j) [p_j] \right\}^{1/2}, \quad (12)$$

where p_i and p_j ($i, j = 1, 2, \dots, 2n + 3$) are the i -th and j -th components of the data vector where the data vector $\mathbf{p} = \{1, (m_{p,1} - m_{p,2}), (m_{p,2} - m_{p,3}), \dots, (m_{p,n-1} - m_{p,n}), (m_{p,1} - m_{p,2})^2, (m_{p,2} - m_{p,3})^2, \dots, (m_{p,n-1} - m_{p,n})^2, i_p, i_p^2, i_p^3, \Delta i_{12}\}$.

The simulated SNe are divided into groups according to their photometric properties. Each training set for a group of SNe consists of the first 100 SNe in that group, assuming that the simulated data are randomly ordered. For groups that contain very small numbers of SNe, we use the first 20 SNe in each group as the training set, or increase the number of SNe used in the training set until no negative z_{phot} results. This led us to a training set containing a total of 1040 SNe used for fitting the analytic photo- z estimator, and a “test set” of 28,662 SNe that are *not* used in the fitting, and are used as a validation set for the analytic photo- z estimator.

In applying the photo- z estimator to simulated data, we find that for each group of SNe with a given set of available photometric passbands, applying a single fitting formulae to its training set may lead to substructure in the estimated z_{phot} . Therefore, we have divided each group into subgroups as shown in Table 1, and derived the photo- z estimator for each subgroup using its own training set. Fig.1 shows $(z_{\text{phot}} - z_{\text{spec}})/(1 + z_{\text{spec}})$ versus z_{spec} (upper panel) and the corresponding histogram of the number of SNe versus $(z_{\text{phot}} - z_{\text{spec}})/(1 + z_{\text{spec}})$ (lower panel), for the analytic photo- z estimator applied to simulated SNe from the LSST, with cut $\sigma_{z_{\text{phot}}}/(1 + z_{\text{phot}}) < 0.1$. The cut is made for better presentation; only 12 SNe out of 1040 of the training set, and 109 out of 28662 of the test set have $\sigma_{z_{\text{phot}}}/(1 + z_{\text{phot}}) \geq 0.1$. Fig.2 is the same as Fig.1, but for imposing the cut $\sigma_{z_{\text{phot}}}/(1 + z_{\text{phot}}) < 0.01$.

Table 2 shows that we can arrive at photo- z 's with higher accuracy, precision, and purity by using the estimated errors on z_{phot} to exclude SNe with large $\sigma_{z_{\text{phot}}}/(1 + z_{\text{phot}})$. If we exclude SNe with $\sigma_{z_{\text{phot}}}/(1 + z_{\text{phot}}) \geq 0.01$, we arrive at a precision of $\sigma(z_{\text{phot}} - z_{\text{spec}})/(1 + z_{\text{spec}}) = 0.02$, a bias in z_{phot} (the mean of $z_{\text{phot}} - z_{\text{spec}}$) of -9×10^{-5} , and an outlier fraction (with $|(z_{\text{phot}} - z_{\text{spec}})/(1 + z_{\text{spec}})| > 0.1$) of 0.23 percent. Note that for the threshold of $\sigma_{z_{\text{phot}}}/(1 + z_{\text{phot}}) < 0.01$, there are no outliers in the training set. We can require that there are no outliers in the training set in order to arrive at this threshold for $\sigma_{z_{\text{phot}}}/(1 + z_{\text{phot}})$.

4.2 Photo-z's using SN Ia colors only

Fig.3 and Fig.4 are results corresponding to Fig.1 and Fig.2, but for z_{phot} obtained using Eq.(7), which uses SN Ia colors only. Using the SN Ia colors only, we obtain a set of photo- z 's with similar quality to using SN Ia color and i band peak flux by requiring that $\sigma_{z_{\text{phot}}}/(1 + z_{\text{phot}}) < 0.007$; this leads to a set of photo- z 's with 2 percent accuracy, a bias in z_{phot} of 5.9×10^{-4} , and an outlier fraction of 0.32%. The threshold level of $\sigma_{z_{\text{phot}}}/(1 + z_{\text{phot}}) < 0.007$ is set naturally by requiring that there are no outliers in the training set.

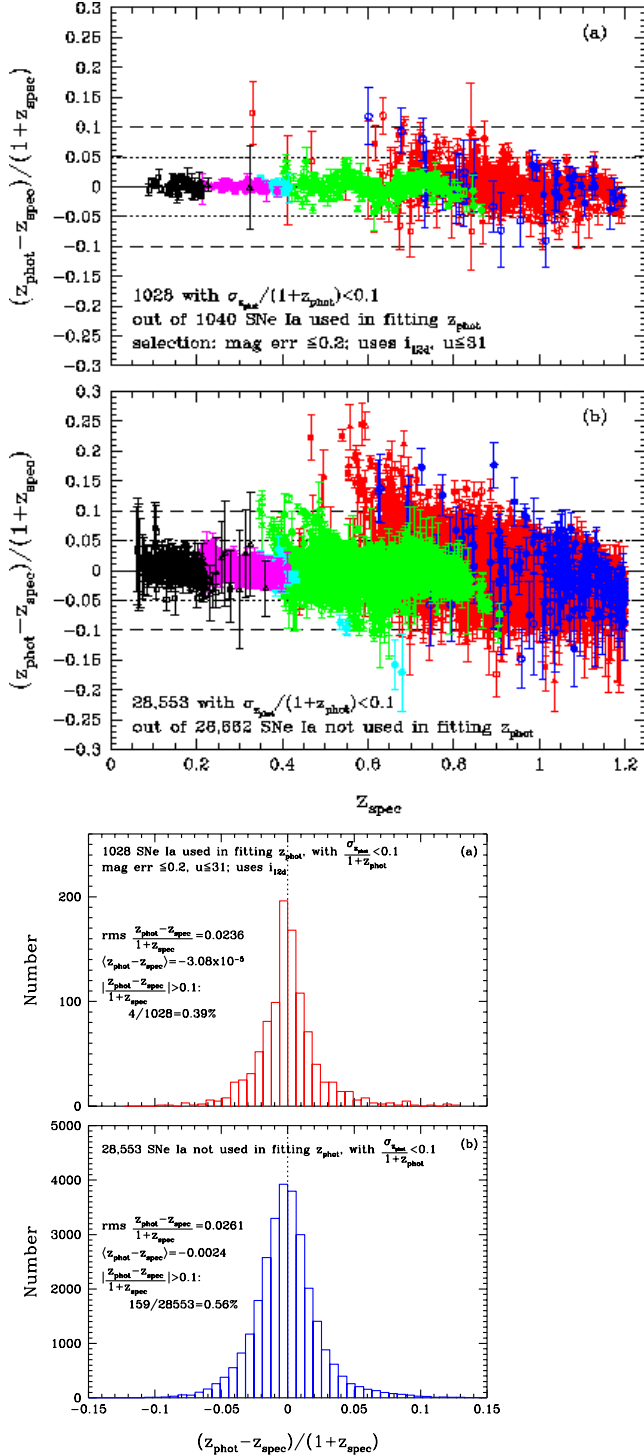


Figure 1. The analytic photo-z estimator applied to simulated SNe from the LSST: $(z_{\text{phot}} - z_{\text{spec}})/(1 + z_{\text{spec}})$ versus z_{spec} (upper panel) and the distribution in $(z_{\text{phot}} - z_{\text{spec}})/(1 + z_{\text{spec}})$ (lower panel), with cut $\sigma_{z_{\text{phot}}}/(1 + z_{\text{phot}}) < 0.1$ for cleaner presentation. Different colors indicate SNe with different photometric passbands, as described in Table 1. For SNe represented by the same color, different point types represent subdivisions based on brightness to improve precision.

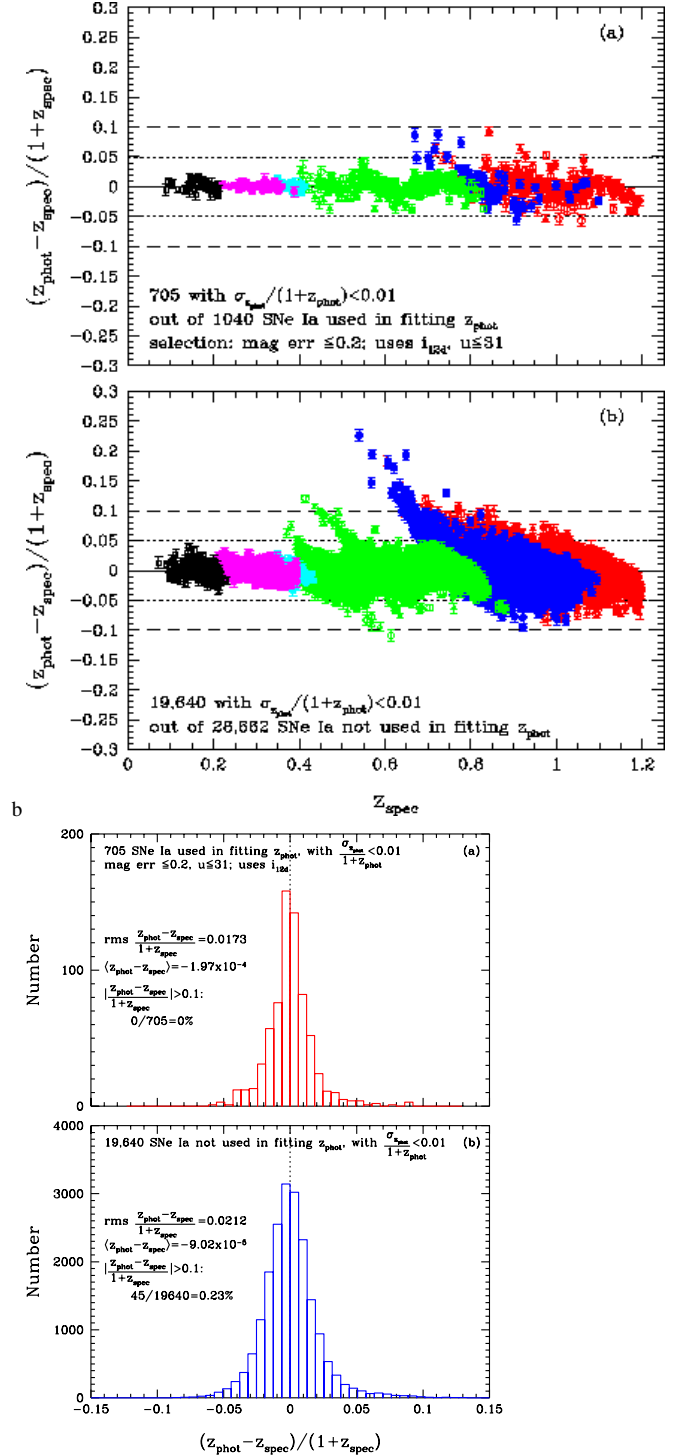


Figure 2. The same as Fig.1, but with cut $\sigma_{z_{\text{phot}}}/(1 + z_{\text{phot}}) < 0.01$ for improved accuracy, precision, and outlier reduction.

5 SUMMARY AND DISCUSSION

We have shown that a simple analytic photo-z estimator for SNe Ia can be built for the LSST, given suitably chosen training sets of SNe Ia with spectroscopic redshifts that are representative of the general properties of SNe Ia from the LSST. While our method is based on that proposed by Wang (2007), and advanced by Wang, Narayan, & Wood-Vasey (2007), it represents a significant

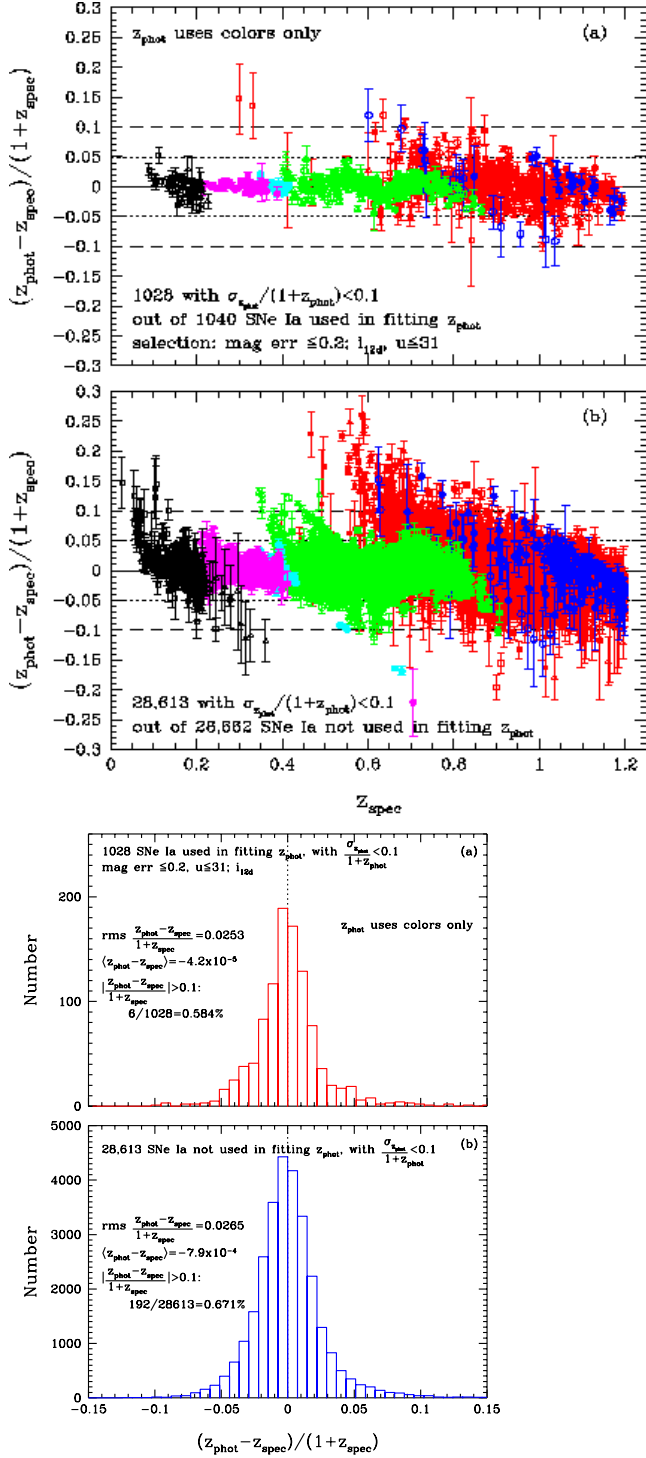


Figure 3. The same as Fig.1, but for z_{phot} obtained using SN Ia colors only.

improvement over previous work (which require the use of both colors and i magnitudes of SNe Ia) in enabling the use of SN Ia colors only. This eliminates the possible complications that can arise from using SN Ia brightness in estimating photo- z 's, since the peak brightness of SNe Ia is already used for measuring distances.

The multiple-band photometry from the LSST enables us to divide the SNe Ia into different sets (see Sec.2.2 and Table 1). For each set, a photo- z estimator is constructed using only quadratic

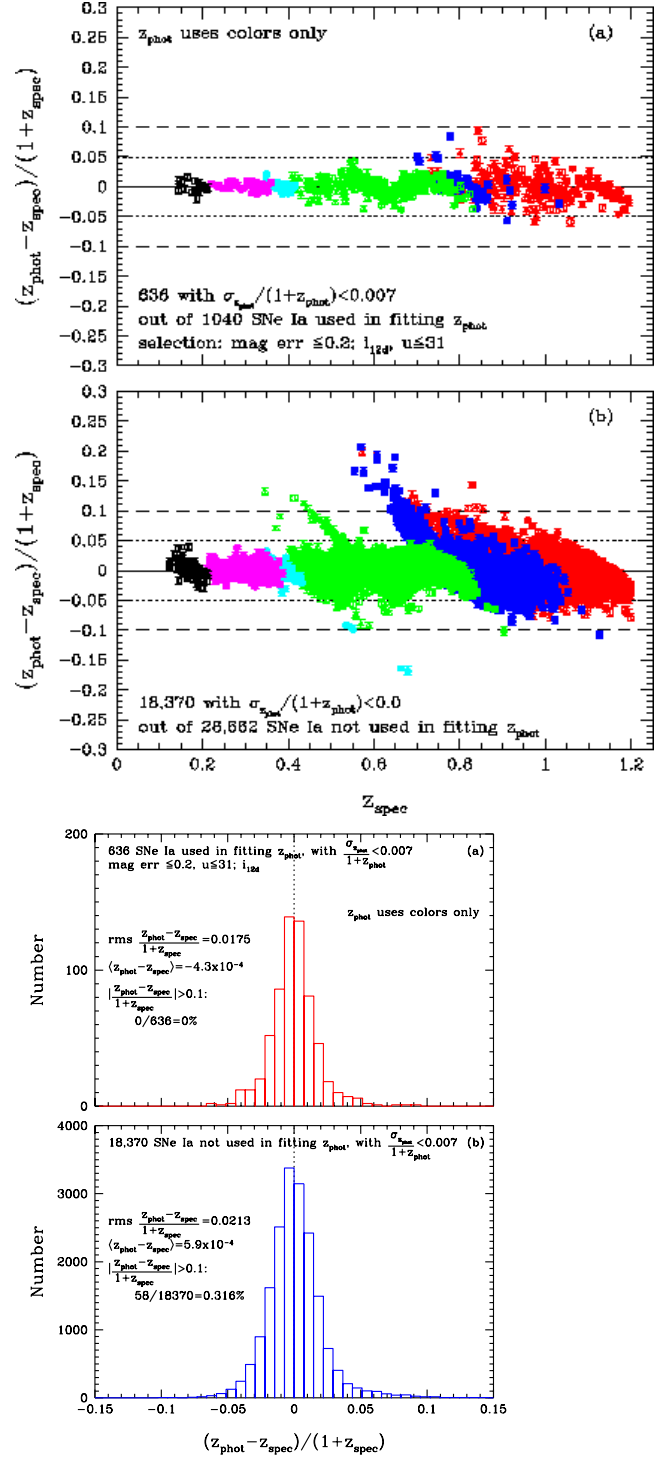


Figure 4. The same as Fig.3, but with cut $\sigma_{z_{\text{phot}}}/(1 + z_{\text{phot}}) < 0.007$ for improved accuracy, precision, and outlier reduction.

functions of colors (see Eq.[7]), with the constant coefficients given by fitting to a training set that contains a maximum of 100 SNe Ia with spectroscopic redshifts (see Table 1).

The performance of our simple analytic SN Ia photo- z estimator is quite impressive when applied to simulated LSST SN Ia photometric data (see Table 2). We find that the estimated errors on the photo- z 's, $\sigma_{z_{\text{phot}}}/(1 + z_{\text{phot}})$, can be used as filters to produce a set of photo- z 's that have high precision, accuracy,

and purity. Using SN Ia colors as well as SN Ia peak magnitude in the i band, we obtain a set of photo- z 's with 2 percent accuracy (with $\sigma(z_{\text{phot}} - z_{\text{spec}})/(1 + z_{\text{spec}}) = 0.02$), a bias in z_{phot} (the mean of $z_{\text{phot}} - z_{\text{spec}}$) of -9×10^{-5} , and an outlier fraction (with $|(z_{\text{phot}} - z_{\text{spec}})/(1 + z_{\text{spec}})| > 0.1$) of 0.23 percent, with the requirement that $\sigma_{z_{\text{phot}}}/(1 + z_{\text{phot}}) < 0.01$. Using the SN Ia colors only, we obtain a set of photo- z 's with similar quality by requiring that $\sigma_{z_{\text{phot}}}/(1 + z_{\text{phot}}) < 0.007$; this leads to a set of photo- z 's with 2 percent accuracy, a bias in z_{phot} of 5.9×10^{-4} , and an outlier fraction of 0.32 percent.

We expect that our SN photo- z estimator for the LSST will be useful in probing dark energy using LSST SNe Ia with photometry only. It will also provide an independent cross-check for SN photo- z 's derived from other, template-based photo- z estimators (see, e.g., Kim & Miquel (2007); Kessler et al. (2010); Palanque-Delabrouille (2010)). Our linear photo- z model is very convenient for propagating photometric uncertainties, especially compared to more “black-box” type machine learning algorithms. In future work, we will examine the cosmological constraints that can be obtained using LSST SNe Ia with photometry only, with photo- z 's estimated using the method presented in this paper.

ACKNOWLEDGMENTS

We are grateful to Michel Wood-Vasey and Alex Kim for helpful discussions, and Kirk Gilmore for an internal review of our paper on behalf of the LSST Dark Energy Science Collaboration. YW was supported in part by NASA grant 12-EUCLID12-0004.

REFERENCES

- Abell, P. A. et al. 2009, e-prints arXiv:0912.0201
 Albrecht, A., et al., Report of the Dark Energy Task Force; available online at arXiv:astro-ph/0609591v1
 Astier, P., et al. 2006, *A & A* 447, 31-48 (2006)
 Bernstein, J.P. et al., *Astrophysical Journal* 753 (2012) 152
 Guy, J. et al. 2007, *Astronomy & Astrophysics*, 466, 11
 Guy, J. et al. 2010, *Astronomy & Astrophysics*, 523, A7
 Kessler, R. et al. 2009a, *ApJS*, 185, 32
 Kessler, R. et al. 2009b, *PASP*, 121, 1028
 Kessler, R. et al., 2010, *ApJ*, 717, 40
 Kim, A. G.; Miquel, R., 2007, *Astroparticle Physics*, 28, 448
 Lupton, R., 1993, “Statistics in Theory and Practice”, Princeton University Press
 Palanque-Delabrouille, N., et al., 2010, *A & A*, 514, A63
 Perlmutter, S., et al., *Astrophysical Journal* 517 (1999) 565
 Riess, A., et al., *Astron.J.* 116 (1998) 109
 Wang, Y. 2007, *ApJ Lett.*, 654, 123
 Wang, Y.; Narayan, G.; Wood-Vasey, M., 2007, *MNRAS*, 382, 377 (2007)

set	bands	subdivision	symbol in Fig.1 & Fig.3	N_s	N_{test}	colors only	$\sigma \left[\frac{\Delta z}{1+z} \right]$ training, test	$\langle z_{\text{phot}} - z \rangle$ training, test	outliers training, test	flagged in test
G11	<i>rizY</i>	$i \geq 24.8$	red filled circles	100	2904	N	.0255, .0299	-2.6E-7, -.0074	0, 22	15
						Y	.0264, .0261	-1.6E-7, -.0032	0, 8	0
G12	<i>rizY</i>	$i = [24.5, 24.8)$	red empty circles	100	3060	N	.0308, .0280	-8.1E-8, -.0039	1, 11	0
						Y	.0313, .0280	-6.0E-7, -.0051	1, 14	0
G13	<i>rizY</i>	$i = [24, 24.5), r \geq 25.2$	red filled triangles	100	4184	N	.0274, .0290	2.5E-7, -.0017	0, 25	0
						Y	.0280, .0289	-1.0E-7, -8.7E-4	1, 26	0
G14	<i>rizY</i>	$i = [24, 24.5), r < 25.2$	red empty triangles	100	1505	N	.0301, .0369	1.1E-7, 3.5E-5	1, 23	4
						Y	.0306, .0362	-6.5E-8, 6.1E-4	1, 22	2
G15	<i>rizY</i>	$i = [23, 24)$	red filled squares	100	4900	N	.0279, .0346	1.1E-7, -8.5E-4	0, 75	0
						Y	.0292, .0352	-3.2E-7, .0021	0, 92	0
G16	<i>rizY</i>	$i < 23$	red empty squares	40	53	N	.0408, .0526	-7.1E-8, -.033	1, 4	2
						Y	.0494, .0612	-2.6E-8, -.039	2, 5	3
G21	<i>izY</i>	$i \geq 24.5$	blue filled circles	20	174	N	.0202, .0472	-1.0E-7, -.0097	0, 6	0
						Y	.0251, .0393	1.4E-8, .0032	0, 3	0
G22	<i>izY</i>	$i < 24.5$	blue empty circles	20	18	N	.055, .108	-1.3E-8, -.068	1, 7	2
						Y	.0627, .0798	4.3E-8, -.0508	2, 5	0
G31	<i>grizY</i>	$i \geq 23.5$	green filled circles	100	2508	N	.0163, .0196	-1.5E-7, .0023	0, 3	2
						Y	.0165, .0192	-3.0E-8, .0035	0, 1	0
G32	<i>grizY</i>	$i = [23.1, 23.5)$	green empty circles	100	3242	N	.0122, .0155	2.1E-7, -.0027	0, 2	0
						Y	.0125, .0157	1.6E-7, -.0016	0, 3	0
G33	<i>grizY</i>	$i < 23.1$	green empty triangles	100	3888	N	.0137, .0179	2.0E-7, -.0069	0, 4	0
						Y	.0151, .0183	-3.8E-8, -.0025	0, 6	0
G4	<i>griz</i>		cyan filled circles	50	480	N	.0055, .0229	2.7E-8, .0018	0, 8	6
						Y	.0059, .0421	-5.7E-8, .0088	0, 11	9
G5	<i>ugriz</i>		magenta filled circles	50	1361	N	.0048, .0094	-1.9E-8, -5.2E-4	0, 1	1
						Y	.0063, .0123	7.2E-8, 9.6E-4	0, 1	0
G61	<i>ugri</i>	$r \geq 21$	black empty triangles	20	75	N	.0049, .048	-1.1E-7, .0091	0, 4	4
						Y	.0097, .0507	-2.1E-8, -.010	0, 4	1
G62	<i>ugri</i>	$r < 21$	black empty squares	40	310	N	.0082, .026	-2.1E-7, .0019	0, 1	1
						Y	.0168, .0319	8.5E-9, .0039	0, 6	1

Table 1. Division of SNe into sets according to available photometric passbands, and into subsets in each set for improved precision. The “outliers” column indicates the number of SNe in the training set and test set that have $|(z_{\text{phot}} - z_{\text{spec}})/(1 + z_{\text{spec}})| > 0.1$. The “flagged in test” column indicates the number of outliers in the test set that have $\sigma_{z_{\text{phot}}}/(1 + z_{\text{phot}}) \geq 0.1$.

set	$\frac{\sigma_{z_{phot}}}{1+z_{phot}} <$	colors only	N_{tot}	N_{cut}	$\sigma \left[\frac{\Delta z}{1+z} \right]$	$\langle z_{phot} - z \rangle$	flagged outlier	outliers
training	100	N	1040	0	.0241	−9.6E-8	0	4
		Y	1040	0	.0259	−1.8E-6	0	7
test	100	N	28662	0	.0270	−.0027	0	196 (0.68%)
		Y	28662	0	.0271	-6.9×10^{-4}	0	207 (0.72%)
training	0.1	N	1028	12	.0236	−3.1E-5	0	4
		Y	1028	12	.0253	−4.2E-5	1	6
test	0.1	N	28553	109	.0261	−.0024	37	159 (0.56%)
		Y	28613	49	.0265	-7.9×10^{-4}	15	192 (0.67%)
training	0.05	N	1011	29	.0229	−.00022	1	3
		Y	1017	23	.0242	−5.1E-4	3	4
test	0.05	N	28327	335	.0257	−.0021	53	143 (0.50%)
		Y	28499	163	.0262	-6.8×10^{-4}	31	176 (0.62%)
training	0.02	N	918	122	.0204	−.00073	3	1
		Y	949	91	.0221	−3.0E-4	5	2
test	0.02	N	26606	2056	.0242	−.0010	95	101 (0.38%)
		Y	27480	1182	.0250	-3.0×10^{-4}	74	133 (0.48%)
training	0.01	N	705	335	.0173	−.00020	4	0
		Y	636	404	.0175	−4.3E-4	7	0
test	0.01	N	19640	9022	.0212	−9.0E-5	151	45 (0.23%)
		Y	18370	10292	.0213	5.9×10^{-4}	149	58 (0.32%)

Table 2. Obtaining sets of photo-z’s with higher accuracy, precision, and purity by using the estimated errors on z_{phot} to exclude SNe with large $\sigma_{z_{phot}}/(1+z_{phot})$.